Analysis and Design of 1-bit Noise-Shaping Quantizer Using Variable Structure Control Approach

Jwusheng Hu and Shiang-Hwua Yu
Department of Electrical and Control Engineering
National Chiao Tung University, Hsinchu, Taiwan

Abstract
This paper introduces a straightforward analysis of a 1-bit noise-shaping quantizer using variable structure control methods. The method using the concept of equivalent control to access the bound on state signals when the sliding condition is reached. Simulation examples and an experimental circuit using off-the-shelf electronic components are given to demonstrate the theoretical analysis.

1. Introduction

Signal quantization is an area that is related to many engineering applications. Among various quantization schemes, sigma-delta modulation is a well-known technique to alter the frequency distribution of quantization noise via the feedback connection of a quantizer with a filter. This technique has various practical uses in data conversion [8] and power conversion [9]. The history of sigma-delta modulation goes back to at least 1952, when de Jager [10] invented the delta modulator for coding analog signals using negative feedback. The delta modulator is a simple feedback system with a one-bit quantizer in the forward path and an integrator in the feedback path. As the name implies, the delta modulator generates the binary signal, which carries information of the differentiation of the input signal. Later, in 1962, Inose, Yasuda and Murakami [11] modified the delta modulator by adding an integrator as a pre-filter, to obtain a modulator which directly carries the information on the input magnitude. This modulator was a prototype of the various sigma-delta modulators of today.

Using a 1-bit quantizer in the feedback loop, the sigma-delta modulator is essentially a nonlinear dynamic system. By far, the most popular method for analyzing a sigma-delta modulator is based on the linear system method, which models the quantizer as a source of additive noise and yields an output noise spectrum determined by the magnitude response of the loop sensitivity function under the white-noise assumption of the quantization error. Accordingly, the sensitivity function is also called the noise transfer function for sigma-delta modulators. However, this is a misnomer, since the white-noise assumption is incorrect [12], and the so-called noise transfer function fails to predict accurately the quantization noise spectrum. In effect, the linear system method cannot explain many of the characteristics of the sigma-delta modulator, especially its stability. Various methods have been used to derive the stability conditions, including for example, norm analysis [13], the describing function method [14][15] and geometrical analysis [16][17][18]. However, all of these methods have deficiencies or limitations, and so can only achieve limited success. Unlike other analysis methods, the theory of sliding modes [6][19], which is a control technique that uses a switching scheme to stabilize a system or to track a signal, seems not to have attracted much attention for its potential in developing a rigorous theory of sigma-delta modulators. The theory of sliding modes was first applied to analyze the stability of the delta and sigma-delta modulator by Sira-Ramirez [20], who mainly considered the first-order case. Zourntos and Johns [21] proposed variable-structure sigma-delta modulators based on the variable structure control with sliding mode; they achieved stability by adapting the loop filter. Alternatively, the sigma delta modulator is essentially a relay feedback system (RFS) with a fast relay switch [4]. Advanced theories and analysis for RFS were investigated in recent years for stability and limit cycle behavior [1][4][5].

The research works on variable structure control and RFS provide a good amount of materials to understand the delta-sigma modulator. However, for practice engineers, a clear design guideline derived from the theory is needed, especially for high-order loop filters. Unfortunately, little works were done (based on variable structure or RFS) to emphasize this need [22][23]. The intention of this work is to introduce a straightforward analysis of 1-bit noise-shaping quantizer based on the well-known variable structure feedback control framework. It is shown that if the loop filter is also stable, global contraction of the state trajectory can be ensured. When the loop filter contains unstable poles (e.g., on the imaginary axis), a state constraint is proposed to allow the state trajectory reach the sliding surface. In practice, all the states have saturation limits (i.e., bounded by supply voltage). Although the sliding condition can still be maintained when some states are saturated, the noise-shaping quantization property is destroyed due to non-linearity. This work also presents an estimation of the state magnitude in practical

0-7803-8335-4/04/$17.00 ©2004 AACC

implementation using a zeroth order holder. Two examples are given to illustrate the design methods.

2. Quantization and Noise Shaping

A general quantization problem can be formulated as,

$$Y_s(s) = H_r(s)R(s) + H_n(s)E(s),$$

where $R(s)$ is the signal to be quantized, $E(s)$ the quantized error and $Y_s(s)$ the quantized result. $H_r(s)$ and $H_n(s)$ are frequency responses of the signal and noise shaping functions. Intuitively, if $E(s)$ is made to be white, selecting $H_n(s)$ is equivalently to shape the quantization noise. For single-bit quantization, $Y_s(s)$ is a bi-level signal and $H_r(s)$ and $H_n(s)$ satisfy,

$$Y_s(s) = \frac{N_2(s)}{N_1(s)}R(s) - \frac{D(s)}{N_1(s)}E(s) \tag{1}$$

where $N_1(s)$, $N_2(s)$ and $D(s)$ are polynomials with $\deg(D) > \deg(N_2)$. Eq.(1) can be rewritten as,

$$E(s) = \frac{N_2(s)}{D(s)}R(s) - \frac{N_1(s)}{D(s)}Y_s(s) = G_2(s)R(s) - G_1(s)Y_s(s) \tag{2}$$

By connecting $E(s)$ and $Y_s(s)$ with a symmetric bi-level quantizer, a 1-bit noise-shaping quantizer can be realized as shown in Figure 1.

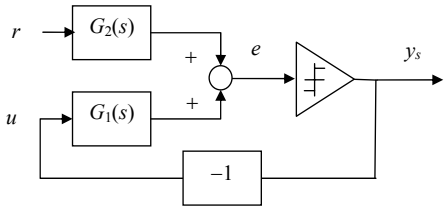

Figure 1. A general 1-bit noise-shaping quantizer where G_1 and G_2 represents the noise and signal shaping function, r the bounded input signal, y_s the output binary sequence

From the control system perspective, the objective of the feedback implementation of Figure 1 is to make e as small as possible by a relay feedback. Let G_1 and G_2 be strictly proper transfer functions and are written as,

$$G_1(s) = \frac{b_{n-1}s^{n-1} + b_{n-2}s^{n-2} + \cdots + b_0}{s^n + a_{n-1}s^{n-1} + a_{n-2}s^{n-2} + \cdots + a_0} \tag{3}$$

and

$$G_2(s) = \frac{d_{n-1}s^{n-1} + d_{n-2}s^{n-2} + \cdots + d_0}{s^n + a_{n-1}s^{n-1} + a_{n-2}s^{n-2} + \cdots + a_0} \tag{4}$$

The input signal r is assumed to be bounded by $\bar{r}$ ($|r| \le \bar{r}$). Consider the minimal state space representation of Figure 1 (Eq.(2)) as,

$$\frac{d}{dt}X = AX + Bu + B_r r,\ e = CX \tag{5}$$

The ability to maintain the output e to be (or around) zero (the so-called *sliding condition*) by using output relay feedback depends on the *order of sliding set* [3]. This degree is defined as the smallest integer m such that $CA^{m-1}B \neq 0$. It has been shown that for $m \ge 2$, the ability to maintain $e = 0$ is very limited (see [1][4]). Therefore, for the quantizer, the selection of the noise shaping function is then restricted to $\deg(D(s)) - \deg(N_1(s)) = 1$ so that $CB \neq 0$ (see Eq.(1)). This in turn means the relative degree of $G_1(s)$ is 1 (i.e., $b_{n-1} \neq 0$ of Eq.(3)).

3. Maintaining Sliding Condition

The behavior of the feedback system under sliding condition can be analyzed by the equivalent control technique. To maintain state trajectory on the sliding surface $e = 0$, the equivalent control of Eq.(5) is [6],

$$u_{eq} = -\frac{1}{CB}CAX - \frac{CB_r}{CB}r \tag{6}$$

As a result, the state trajectory under the sliding condition is governed by the following dynamic,

$$\frac{d}{dt}X = \left(I - \frac{BC}{CB}\right)AX + \left(I - \frac{BC}{CB}\right)B_r r \tag{7}$$

The following facts can be derived from standard control theory practice [2].

Fact 1: the characteristic equation of the state transition matrix of Eq.(7) is

$$\lambda\left(b_{n-1}\lambda^{n-1} + b_{n-2}\lambda^{n-2} + \cdots + b_0\right) = 0.$$

Fact 2: the transfer function from input r to a signal $\eta = CAX$ is,

$$G_s(s) = CA\left(sI - \left(I - \frac{BC}{CB}\right)A\right)^{-1}\left(I - \frac{BC}{CB}\right)B_r, \tag{8}$$

which is not minimal with at least a pole-zero cancellation at $s = 0$.

From Fact 1, it is obvious that to have a sliding condition, the zeros of $G_1(s)$ must be stable. This guarantees a bounded state trajectory when sliding occurs. Fact 2 ensures that $G_s(s)$ is stable and its l_1-norm exists. The static switching control feedback of Figure 1 can be written as,

$$u = -y_s = -\frac{1}{CB}\bar{U}sign(e),\ \ \bar{U} > 0. \tag{9}$$

It is then necessary to find out the magnitude of $\bar{U}$ to maintain the sliding condition. Consider the energy function $V_e = \frac{1}{2}e^2$. The derivative of V_e is,

$$\frac{d}{dt}V_e = -\left(\bar{U} - \eta \cdot sign(e) - CB_r r \cdot sign(e)\right)|e|, \text{ where } \eta = CAX. \tag{10}$$

Therefore, to trap e on the sliding surface (e=0), a conservative estimate of the minimum magnitude $\bar{U}$ is,

$$\bar{U} \ge |\eta| + |CB_r| \cdot \bar{r}. \tag{11}$$

where $\bar{r}$ denotes the maximum amplitude of r. The signal η is actually the output of Eq.(7) and its magnitude when the states are trapped on the sliding surface is estimated as,

$$|\eta| \le \|G_s(s)\|_1 \bar{r} \tag{12}$$

where $\|\cdot\|_1$ denotes the l_1-norm. The following lemma summarizes the analysis.

Lemma 1: the sliding condition e=0 of Eq.(5) under the feedback of Eq.(9) can be maintained if the following conditions are satisfied:

(1.) The relative degree of $G_1(s)$ is 1 and all the zeros

are stable.

(2.) $\bar{U} \geq \left(\|G_s(s)\|_1 + |CB_r|\right)\cdot \bar{r}$

Note that Lemma 1 says nothing about stability of the feedback system under arbitrary initial conditions. Once $\bar{U}$ is determined and satisfies Lemma 1, the state trajectory will stay inside a bounded set called *sliding region* as,

$$S = \left\{X \middle| X \in R^n,\ |CAX| < \bar{U} - |CB_r|\cdot \bar{r} \text{ and } CX = 0\right\} \quad (13)$$

Another important issue regarding practical implementation is to ensure that all the states stay within their saturation limits. Checking whether the saturation limits are exceeded can be done by investigating the l_1-norm of the transfer function for each state on the sliding region (Eq.(13)).

4. Convergence to Sliding surface

It is important to know the sets of initial conditions which guarantee the sliding condition. In this paper, a practical view point is taken by constraining the state to ensure sliding condition.

4.1 Stable Open Loop Filter

For a stable open loop filter, it is possible to establish a global contraction region of the system (Figure 1). When $G_1(s)$ satisfies condition (1.) in Lemma 1 and is stable (all poles on the open LHP), $G_1(s)$ is also strictly positive real (SPR). The Kalman-Yacubovich lemma [7] states that there exists P and Q, both positive definite and symmetric, such that

$$A^{\mathrm{T}}P + PA = -Q \text{ and } PB = C^{\mathrm{T}}. \quad (14)$$

Define $V = 0.5X^T PX$, we have,

$$\frac{d}{dt}V = -\frac{1}{2}X^T QX + X^T PBu + X^T PB_r r$$

By Eq.(5), we have

$$\frac{d}{dt}V = -\frac{1}{2}X^T QX - (CB)^{-1}\bar{U}|e| + X^T PB_r r \quad (15)$$

Let $Q = W^{\mathrm{T}}W$ and $PB_r = W^{\mathrm{T}}q$, Eq.(15) can be rewritten as,

$$\frac{d}{dt}V = -\frac{1}{2}(WX - rq)^T(WX - rq) + r^2 q^T q - (CB)^{-1}\bar{U}|e| \quad (16)$$

Define the following three sets:

$$\Omega_y = \left\{X \middle| X \in R^n,\ |CX| \leq \frac{1}{\bar{U}}r^2 q^T q\right\}, \quad (17)$$

$$\Omega_r = \left\{X \middle| X \in R^n, \|WX - rq\| \leq |r|\|q\|\right\}, \quad (18)$$

$$\Omega_\rho = \left\{X \middle| X \in R^n, X^T PX \leq \rho, \rho \geq 0\right\}. \quad (19)$$

It can be shown that for finite r, Ω_r is finite since W is non-singular. We can establish the invariant contraction region of the state X in the following lemma.

Lemma 2: if the transfer function between u and e in Eq.(5) is strictly positive real, $\Omega_{\bar{\rho}}$ is an invariant contraction region of the states under the feedback of Eq.(9) where

$$\bar{\rho} = \underset{\rho}{Min}\left\{\Omega_\rho \supseteq \left\{\bigcup_{|r|\leq \bar{r}} \Omega_r \cap \Omega_y\right\}\right\}.$$

[Proof]: Since for every $X \notin \Omega_{\bar{\rho}}$, we have $\dot{V} < 0$ from Eq.(16). ■

The contraction region states nothing about entering the sliding surface. Consider $e(0) > 0$ so we have $u(0) = -\bar{U}/CB$. If no switching happens, the steady state response of Figure 1 becomes,

$$e_{ss}(t) = -CA^{-1}B\frac{\bar{U}}{CB} + \int_0^t g_2(t-\tau)r(\tau)d\tau \quad (20)$$

If the signs of both $CA^{-1}B$ and CB are the same, the response is less and equal to zero if,

$$\bar{U} \geq \left|\frac{CB}{CA^{-1}B}\right|\|G_2(s)\|_1 \bar{r}\,. \quad (21)$$

As a result, the switching must occur. Similar analysis can be shown when $e(0) < 0$. The trajectory will stay on the sliding surface if it hits the sliding region (Eq.(13)). Note that Eq.(21) is a sufficient condition considering a general bounded input r. If r=0, for example, switching will happen when the signs of both $CA^{-1}B$ and CB are the same, regardless of the magnitude of $\bar{U}$.

A simple geometrical interpretation can be shown to illustrate the stability condition. First observe that $\bigcup_{|r|\leq \bar{r}} \Omega_r \subset \bigcup\{\Omega_{\bar{r}}, \Omega_{-\bar{r}}\}$. To see this, consider the following inequalities.

For $0 \leq r \leq \bar{r}$,

$$\|WX - \bar{r}q\| = \|WX - rq + (r - \bar{r})q\| \leq \|WX - rq\| + |r - \bar{r}|\|q\|,$$
$$\leq |r|\|q\| + |r - \bar{r}|\|q\| = |\bar{r}|\|q\|$$

and for $-\bar{r} \leq r \leq 0$,

$$\|WX + \bar{r}q\| = \|WX - rq + (\bar{r} + r)q\| \leq \|WX - rq\| + |\bar{r} + r|\|q\|.$$
$$\leq |r|\|q\| + |\bar{r} + r|\|q\| = |\bar{r}|\|q\|$$

Figure 2 depicts various sets (Eqs.(17)-(19)), sliding surface and sliding region for a 2nd order system. The illustration shows that the sliding surface within the invariant set is also sliding region.

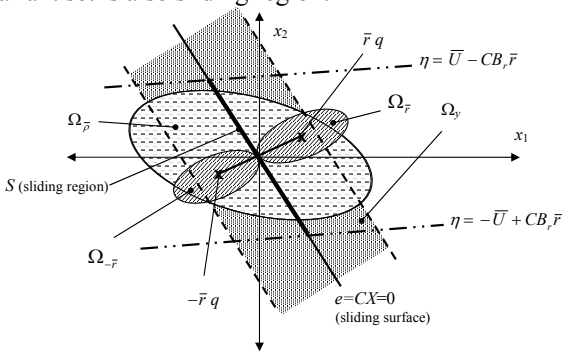

Figure 2 Geometric interpretation of Lemma 2

4.2 Constraining the State

For a more general case where the open loop filter could be unstable, a state constraint is proposed in this paper to ensure sliding condition. From Eqs.(10) and (11), the

energy function V_e can be made decreasing if the magnitude of η=CAX is bounded. Assume that the bound is possible and is equal to $\overline{\eta}$. The state trajectory will eventually hit the sliding surface and stay on the surface if

$$\overline{U} \ge \overline{\eta} + |CB_r| \cdot \bar{r} \tag{22}$$

In addition, Fact 1 and 2 are applied if η does not reach the bound $\overline{\eta}$ when staying on the sliding surface. Therefore, using the concept of equivalent control (Eqs.(6) - (8)), we have,

$$\overline{\eta} \le \|G_s(s)\|_1 \bar{r} \tag{23}$$

One possibility of imposing the limit on η is to make η a physical signal in implementation. For example, consider the canonical form of Eq.(5) as,

$$\frac{dX}{dt} = \begin{bmatrix} 0 & 1 & 0 & \cdots & 0 \\ 0 & 0 & 1 & \cdots & 0 \\ \vdots & \vdots & \ddots & \ddots & \vdots \\ 0 & 0 & \cdots & 0 & 1 \\ -a_0 & -a_1 & \cdots & -a_{n-2} & -a_{n-1} \end{bmatrix} X + \begin{bmatrix} b_{n-1} \\ b_{n-2} \\ \vdots \\ b_1 \\ b_0 \end{bmatrix} u + \begin{bmatrix} d_{n-1} \\ d_{n-2} \\ \vdots \\ d_1 \\ d_0 \end{bmatrix} r,$$

$$e = \begin{bmatrix} 1 & 0 & \cdots & 0 \end{bmatrix} X = x_1 \tag{24}$$

The signal η is actually the state x_2.

5. Practical Design Issues

In reality, however, it is impossible to have a switch acting infinitely fast as assumed in previous sections. One of the applications of sigma-delta modulator is to perform analog-to-digital conversion where a sample-and-hold function is added (Figure 3).

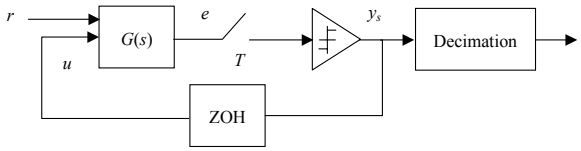

Figure 3 An A/D conversion using sigma-delta modulation where T is the sampling period

Now the switching action of Eq.(9) becomes,

$$u(\tau) = -y_s = -\frac{1}{CB}\overline{U} sign(e((k-1)T)), \quad \forall \ (k-1)T \le \tau < kT$$

$$\overline{U} > 0. \tag{25}$$

Let $e(k) = e(kT)$, from Eq.(5),

$$e(k) - e(k-1) = \int_{(k-1)T}^{KT} C\dot{X}(\tau) d\tau = \int_{(k-1)T}^{KT} (CAX + CB_r r) d\tau - T\overline{U} sign(e(k-1)) \tag{26}$$

$$= T\left(CAX(k-1) + CB_r \bar{r} - \overline{U} sign(e(k-1)) + \xi\right)$$

where ξ is of order T, i.e., $\xi = O(T)$. Therefore,

$$e(k-1)\left(e(k) - e(k-1)\right) = T\left[sign(e(k-1))\left(CAX(k-1) + CB_r \bar{r} + \xi\right) - \overline{U}\right] e(k-1) \tag{27}$$

For a sufficiently small T, it is possible to have a $\overline{U}$, larger than the optimal estimate of Eq.(13), which makes Eq(27) less than zero when $e(k-1)\neq 0$. As a result, we have $|e(k)| < |e(k-1)|$ when $e(k-1)\neq 0$. In other words, $e(k)$ will be trapped in a bounded region (so-called chattering). Referring to Eq.(26), the worst-case increment of $e(t)$ is,

$$|e(t) - e(k-1)| \le T\left[\underset{(k-1)T \le \tau < kT}{Max} |\eta(\tau)| + |CB_r| \cdot \bar{r} + \overline{U}\right].$$

$$\approx 2T\overline{U}, \ \forall \ (k-1)T \le t < kT$$

Since $e(k)$ is decreasing, the bound of $e(t)$ can be estimated as,

$$|e(t)| \le 2T\overline{U} \tag{28}$$

Eq.(28) not only gives an estimate of the chattering amplitude, but also reveals that the amplitude is proportional to the amplitude of the switch. In other words, a good choice of $\overline{U}$ is very important to minimize the size of chattering which affects the S/N ratio of the conversion.

6. Simulation and Experiment

Example 1:

A 4-th order stable loop filter is considered ($G_1(s)$ in Eq.(2)) as:

$$G_1(s) = \frac{N_1(s)}{D(s)} = \frac{s^3 + 2.52\times10^5 s^2 + 3.16\times10^{10} s + 1.98\times10^{15}}{(s + 6.28)^4}. \tag{29}$$

$N_1(s)$ is the denominator of a 3-rd order Butterworth lowpass filter with cutoff frequency at 20 KHz. The input signal is assumed to be bounded by 1 ($\bar{r} = 1$) and the input channel is the same as the feedback (i.e., $N_1(s) = N_2(s)$ in Eq.(1) or $B_r = B$ in Eq.(5)). It can be verified that when $B_r = B$, the transfer function $G_r(s) = 0$ (Eq.(5)). Further, we have,

$CB = 1$, $CA^{-1}B = -1.27\times10^{12}$ and $\|G_2(s)\|_1 = \|G_1(s)\|_1 = 1.27\times10^{12}$.

Therefore, the lower bound of feedback parameter $\overline{U}$ to maintain the sliding condition is (Eq.(11)),

$$\overline{U} \ge 1 \tag{30}$$

The same lower bound can also be computed to ensure switching (Eq.(21)). A simulation is conducted using the digital implementation (Figure 3) with the sampling frequency 1000 KHz (50 times the bandwidth of 20 KHz). The gain $\overline{U}$ is selected to be 2. Using Eq.(28), the error $e(t)$ is bounded as,

$$|e(t)| \le 2T\overline{U} = 4\times10^{-6}$$

This value is then used as the estimate of the quantization error bound (Eq.(1)). Figure 4 shows the spectrum of the simulation result. Note that the quantization error is pushed into the high frequency range and the theoretical prediction is quite accurate.

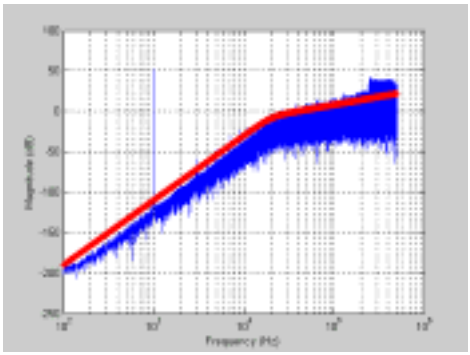

Figure 4 Spectrum of the binary sequence for 1 KHz

sinusoidal reference signal in Example 1 and theretical prediction of the quantization error spectrum

Example 2:

In this example we consider implementing a 4-th order loop filter as,

$$G_1(s)=\frac{N_1(s)}{D(s)}=\frac{9.85\times10^5(s^3+4.93\times10^5 s^2+1.42\times10^{11}s+2.05\times10^{16})}{s^4} \quad (33)$$

and

$$G_2(s)=\frac{N_2(s)}{D(s)}=\frac{1.01\times10^{22}}{s^4}$$

Figure 5 shows the schematic circuit of the sigma-delta modulation. The comparator's bandwidth limitation is equivalent to 2.8571 MHz sampling frequency as dipicted in Figure 3.

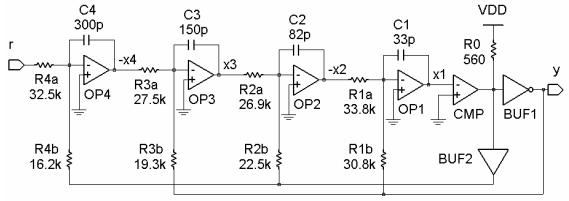

Figure 5 Circuit realization of a 4th-order sigma-delta modulator in Example 2 (CMP: comparator; VDD: 5 Volts)

The circuit implementation of Figure 5 gives the following state-space representation where the states are the voltages of the operational amplifiers.

$$\frac{dX}{dt}=\begin{bmatrix}0 & 895570 & 0 & 0\\ 0 & 0 & 452940 & 0\\ 0 & 0 & 0 & 242510\\ 0 & 0 & 0 & 0\end{bmatrix}X+\begin{bmatrix}985130\\ 541820\\ 345150\\ 205330\end{bmatrix}u+\begin{bmatrix}0\\ 0\\ 0\\ 102670\end{bmatrix}r, \quad (35)$$

$$e=\begin{bmatrix}1 & 0 & 0 & 0\end{bmatrix}X=x_1$$

The corresponding parameters are computed as,

$CB = 985130$, $CB_r = 0$ and $\|G_s(s)\|_1 = 6.07\times10^5$.

From Figure 5, the maximum amplitude of the input signal r is restricted to the circuit supply voltage VDD = 5 Volts (i.e., $\bar{r}=5$). Considering again a bounded input reference signal, from Eqs.(11) and (12), we have,

$\bar{U} \geq 3.04\times10^6$

If this lower bound is used, the feedback control law is (Eq.(9)),

$$u=-3.09\times sign(e). \quad (36)$$

Secondly, since the loop filter is not stable, it is necessary to constrain the variable $\eta = CAX$ (see Section 4.2). From Eqs. (23) and (35),

$$|\eta| = 895570|x_2|\times VDD \leq 3.04\times10^6 \Rightarrow |x_2| \leq 3.39 \quad (37)$$

The bounds of x_3 and x_4 on the sliding surface can also be computed as,

$$|x_3| \leq 4.05 \text{ and } |x_4| \leq 4.56 \quad (38)$$

The results of Eqs.(36) to (38) shows that the state signals do not exceed the supply voltage limit. Figure 5 shows a simplified implementation in which both the switching control gain (Eq.(36)) and the state constraint (Eq.(37)) are,

$$u=-5.0\times sign(e) \text{ and } |x_2| \leq 5.0. \quad (39)$$

As a result, the error e (or x_1) is bounded by (Eq.(28)),

$$|e(t)|=|x_1(t)| \leq 2T\bar{U}=3.45 \quad (40)$$

Assuming all components of Figure 5 are ideal, simulation using the control law (Eq.(39)) and 2.8571 MHz sampling frequency was conducted and the time sequence of each states are plotted in Figure 6. In the simulation, a non-zero initial condition of $X = [5.0\ -5.0\ 7.0\ 9.0]^T$ is applied (not on the sliding surface). It is shown that the system is stable and all state signals stays within the saturation limit of 5 volts. Figure 7 shows the signal of x_2 at initial stage. Notice that it hits the saturation limit initially but becomes stable afterwards.

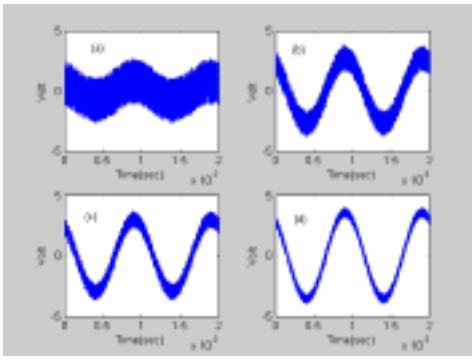

Figure 6 State signals (steady state) of Example 2 where the input is a 1 KHz sin signal and the initial condition is $X=[5.0\ -5.0\ 7.0\ -9.0]^T$; (a) x_1; (b) x_2; (c) x_3; (d) x_4

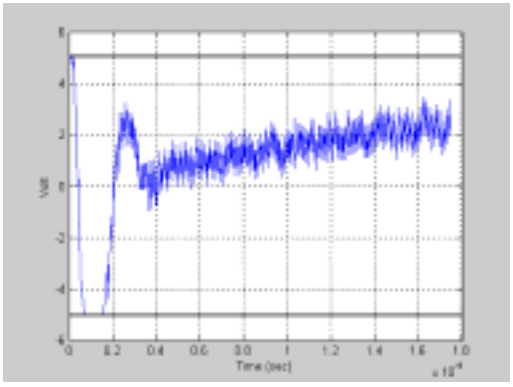

Figure 7 The signal of x2 in Example 2 at initial stage (hitting the saturation limit (±5V) but become stable afterwards)

The circuit of Figure 5 was implemented using off-the-shelf electronic components. Figure 8 shows the state signals of the experiment. It verifies that the system is stable and all states stays withing the saturation limit. However, notice that the signals are smoother than the simulation (Figure 6) because the electronic components are not ideal and cannot act infinitely fast.

7. Conclusion

An analysis of 1-bit noise-shaping quantizer using variable structure control methods is presented. The method using the concept of equivalent control to access the bound on state signals when the sliding condition is reached. For a stable loop filter, the global stability can be proved using the Lyanpunov stability theory. For an unstable loop filter,

the paper proposes a state constraint approach to ensure the sliding condition. Simulation examples and an experimental circuit using off-the-shelf electronic components are given to demonstrate the theoretical analysis.

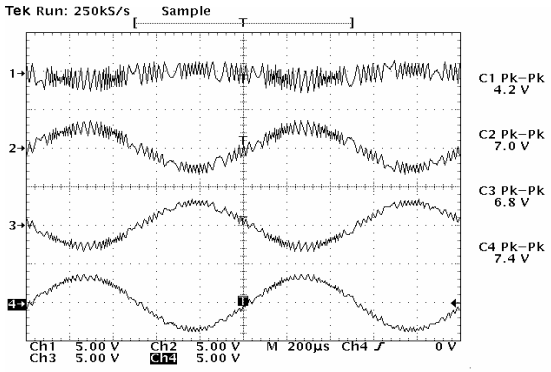

Figure 8 State signals of the experimental circuit (C1 to C4 represents states x_1 to x_4; PK-PK means peak-to-peak)

Reference

[1] Karl Henrik Johansson, "Relay Feedback and Multivariable Control," doctoral dissertation, Department of Automatic Control, Lund Institute of Technology, October 1997.

[2] Kailath, T., *Linear Systems*, Prentice Hall, Englewood Cliffs, New Jersey, 1980.

[3] L. M. Fridman and A. Levant, "Higher order sliding modes as a natural phenomenon in control theory," in *Robust Control via Variable Structure & Lyapunov Techniques*, F. Garofalo and L. Glielmo, Eds. New York: Springer-Verlag, 1996, vol. 217, Lecture notes in control and information science, pp. 107–133.

[4] Karl Henrik Johansson, Andrey E. Barabanov, and Karl Johan Åström, "Limit Cycles with Chattering in Relay Feedback Systems," in *IEEE Transactions on Automatic Control*, vol. 47, no. 9, September 2002.

[5] Jorge M. Gonçalves, Alexandre Megretski, and Munther A. Dahleh, "Global Stability of Relay Feedback Systems," *IEEE Transactions on Automatic Control*, VOL. 46, NO. 4, APRIL 2001.

[6] V. I. Utkin, *Sliding Modes in Control Optimization*, Berlin, Germany, Springer-Verlag, 1992.

[7] M. Vidyasagaar, *Nonlinear Systems Analysis*, Prentice-Hall, Inc., Englewood Cliffs, New Jersey, 1978.

[8] R.W. Adams, P.F. Ferguson, A. Ganesan, S. Vincelette, A. Volpe and R. Libert, "Theory and practical implementation of a fifth-order sigma-delta A/D converter," *J. Audio Eng. Soc*., vol. 39, pp. 515-528, 1991.

[9] J. F. Silva, "PWM audio power amplifiers: sigma delta versus sliding mode control," *IEEE Int. Conference on Electronics, Circuits and Systems*, vol. 1, pp. 359-362, 1998.

[10] F. de Jager, "Delta modulation—a method of PCM transmission using the one unit code," *Philips Res. Repts*., Vol. 7, pp. 442-466, 1952.

[11] H. Inose, Y. Yasuda, and J. Murakami, "A telemetering system by code modulation— $\Delta - \Sigma$ modulation," *IRE trans. on Space Electronics and Telemetry*, vol. SET-8, pp. 204-209, 1962.

[12] R.M. Gray, "Quantization noise in $\Delta\Sigma$ A/D converters," in *Delta-Sigma Data Converter*: *Theory, Design and Simulation*, S.R. Norsworthy, R. Schreier and G.C. Temes, eds. IEEE Press, 1997.

[13] R. Schreier and Y. Yang, "Stability tests for single-bit sigma-delta modulators with second-order FIR noise transfer functions,' *Proc. IEEE Int. Symp. Circuits and Systems*, pp. 1316-1319, 1992.

[14] R.T. Baird and T.S. Fiez, "Stability analysis of high-order delta-sigma modulation for ADC's," *IEEE Trans. Circuits and Systems-II*, vol. 41, no. 1, pp. 59-61, 1994.

[15] J. van Engelen and R. van de Plassche, "New stability criteria for the design of lowpass sigma-delta modulators," in *Proc. of Int. Symp. On Low Power Electronics and Design,* pp. 114-118, 1997.

[16] H. Wang, "A geometric view of $\Sigma\Delta$ Modulations," *IEEE Trans. Circuits and Systems-II*, vol. 39, no. 2, pp. 402-405, 1992.

[17] S. Hein and A. Zakhor, "On the stability of sigma delta modulators," *IEEE Trans. Signal Processing*, vol. 41, no. 7, pp. 2333-2348, 1993.

[18] R. Farrell and O. Feely, "Bounding the integrator outputs of second-order sigma-delta modulators," *IEEE Trans. Circuits and Systems-II*, vol. 45, no. 6, pp.691-702, 1998.

[19] J.Y. Hung, W. Gao, and J.C. Hung, "Variable structure control: a survey," *IEEE Trans. Industrial Electronics*, vol. 40, no. 1, pp. 2-22, 1993.

[20] H. Sira-Ramirez, "Analog signal encoding in delta modulation circuits using the theory of variable structure systems," in *Proc. of the 27th IEEE conference on Decision and Control*, vol. 2, pp. 940-945, 1988.

[21] T. Zourntos and D.A. Johns, "Variable-structure compensation of delta-sigma modulators: stability and performance," *IEEE Trans. Circuits and Systems-I*, vol. 49, no. 1, pp. 41-51, 2002.

[22] Sergey Plekhanov, Ilya A. Shkolnikov, and Yuri B. Shtessel, "High Order Sigma-Delta Modulator Design via Sliding Mode Control," *Proceedings of the American Control Conference*, Denver, Colorado June 4-6, 2003.

[23] Shiang-Hwua Yu and Jwu-Sheng Hu, "Analysis and Design of a Single-Bit Noise-Shaping Quantizer," *Proceedings of the American Control Conference*, Denver, Colorado June 4-6, 2003.